A New Critical State-Based Constitutive Model in Multilaminate Framework

Hamid Karimpour
Stantec Consulting Ltd., Calgary, Alberta, Canada

ABSTRACT
A new constitutive model based on critical state theory is introduced to model behavior of granular material. This new model is a bounding surface plasticity model in multilaminate framework that allows capturing the effects of inherent and induced anisotropy as well as principal stress rotation. Multilaminate framework is a tool and cannot predict the behavior of material independently from a constitutive model. Multilaminate framework is semi-micromechanical tool based on formulating a number of planes with varying orientations over a virtual unit sphere around a stress point.
The constitutive equations of the model are derived within the context of non-linear elastic behavior and plastic sliding of interfaces of predefined planes from multilaminate framework. Presented here are multilaminate framework details, the constitutive equations of the original bounding surface model in the multilaminate framework and sensitivity analysis of key material parameters that clearly show the capabilities and flexibility of the presented constitutive model in predicting drained and undrained behavior of granular material.

RÉSUMÉ
Un nouveau modèle constitutif basé sur la théorie de l'état critique est introduit pour modéliser le comportement de matériaux granulaires. Ce nouveau modèle est un modèle de consistance de surface limite dans un cadre multi-laminé qui permet de capturer les effets de l'anisotropie inhérente et induite ainsi que la rotation de stress principale. Le cadre multi-laminé est un outil et ne peut pas prédire le comportement de matériaux de manière indépendante à partir d'un modèle constitutif. Le cadre multi-laminé est un outil semi-micromécanique basé sur la formulation d'un certain nombre de plans avec des orientations différentes sur une sphère d'unité virtuelle autour d'un point de stress.
Les équations constitutives du modèle sont dérivées dans le contexte du comportement élastique non-linéaire et du glissement plastique des interfaces des plans prédéfinis à partir du cadre multi-laminé. Nous présentons ici les détails du cadre multi-laminé, les équations constitutives du modèle de surface limite original dans le cadre multi-laminé et l'analyse de sensibilité des paramètres matériels clés qui montrent clairement les capacités et la flexibilité du modèle constitutif présenté pour prédire le comportement drainé et non drainé de matériaux granulaires.

1 INTRODUCTION

A numerous number of constitutive models have been presented with different capabilities, mostly based on experimental observations of material behavior using elasticity and plasticity theories. Usefulness of these models will be based on various factors such as soil grading and texture, presence of water, loading condition, etc. To name a few, the following researchers have introduced classic constitutive models that have been widely used in geotechnical engineering: Drucker et al. (1957), Roscoe and Burland (1968), DiMaggio and Sandler (1971), Lade (1977), Prevost (1978), Mroz et al. (1981), Ghaboussi and Momen (1982), Desai and Faruque (1984), Poorooshasb and Pietruszak (1985), Dafalias and Herrmann (1986).

Taylor (1938) presented a framework referred to as multilaminate. Multilaminate framework is semi-micromechanical tool based on formulating a number of planes with varying orientations over a virtual unit sphere around a stress point. A weight factor is assigned to each plane with respect to the volume of the unit sphere. The overall response of the material when subjected to a load will then be integrated by summation of the contributions of all planes.

Multilaminate framework is a tool and cannot predict the behavior of material independently. A constitutive law can be defined in this framework to take advantage of its features. By using this framework the overall behavior is, obtained by accumulating responses of the defined planes. Mathematically, any constitutive law could be used in this framework.

Batdrof and Budiansky (1949) presented a multilaminate plasticity theory for metals that considered development of plastic shear strain along the direction of the shear stress path component.

Zienkiewicz and Pande (1977) used Batdrof and Budiansky's constitutive model and expanded it to fractured rocks. A similar approach was also employed by Pande and Pietruszczak (1982) for prediction of liquefaction of layered sand called reflecting surface model. In the same framework, Bazant and Oh (1983) presented a new model referred to as micro-plane for analyzing cracking in concrete. Pande and Pietruszczak (2001) provided a multilaminate model to describe soil anisotropy. Schweiger et al. (2009) provided a multilaminate model capable of considering both induced and inherent anisotropy for soils.

An existing bounding surface constitutive model, as proposed by Crouch et al. (1994) based on Dafalias and Herrmann (1986), is explained in the multilaminate framework to introduce a new constitutive model. In this article, details of the new constitutive model is presented. In addition, a sensitivity analysis has been performed on

the most influential material parameters to show the capabilities and flexibility of the constitutive model in capturing drained and undrained behavior of granular materials.

2 MULTILAMINATE FRAMEWORK

Using a multilaminate model, one could define a numerical relation between the microscopic and macroscopic behaviours. An existing bounding surface constitutive model, as proposed by Crouch et al. (1994) and referred to as unified critical state bounding model has been defined in the multilaminate framework.

The original bounding surface constitutive model uses two different radial and deviatoric mapping rules to define the loading surface based on the failure surface. Also, an innovative approach, based on movement of the mapping center are used in this model to observe the rotation of the principal stress axes and account for imposed anisotropy effects. The intrinsic anisotropy and bedding effects can be considered when using the multilaminate model by defining different material parameters on different planes.

2.1 Definition of Planes and Local Coordinates

To satisfy conditions of the multilaminate framework from the engineering viewpoint and reduce high computational costs, a limited number of sampling planes are used. Considering a good distribution of plastic deformation and avoiding high computing time, the choice of 13 independent planes as shown in Figure 1 is a fair number for solution of any three-dimensional problem.

The components of the unit normal vector of plane i (l_i, m_i and n_i) and plane's weight coefficients (w_i) for the numerical integration rule are presented in Table 1. The coefficients w_i have been calculated based on Gauss Quadrature numerical integration rule. The presented w_i are acceptable for a first order tensor and are corrected for a second order tensor like (e.g., stress or strain) by multiplying the ratio of area for each plane on the unit sphere.

A coordinate system has been used for each plane such that one axis is perpendicular to the plane and two axes are on the plane. Plastic shear strains are considered on the planes.

2.2 Stress and Strain Vectors

In the following equations { } and [ ] denote a 9-element vector and a square matrix, respectively. Superscript T indicates a transposed array. A superposed dot indicates the rate and | | refers to the norm. Following this notation $|\{\ \}|$ is the length of a vector whereas $\{|\ \ |\}$ represents a unit vector ($\{|\ \ |\} = \{\ \}/|\{\ \}|$). A comma followed by a subscripted variable implies the partial derivative with respect to that variable. Bars over the stress quantities refer to points on the bounding surface. The effective stress, strain and Kronecker's delta vectors are defined as follows:

$$\begin{aligned}\{\varepsilon\} &= \{\varepsilon_{11}\ \ \varepsilon_{22}\ \ \varepsilon_{33}\ \ \varepsilon_{12}\ \ \varepsilon_{21}\ \ \varepsilon_{13}\ \ \varepsilon_{31}\ \ \varepsilon_{23}\ \ \varepsilon_{32}\}^T \\ \{\sigma\} &= \{\sigma_{11}\ \ \sigma_{22}\ \ \sigma_{33}\ \ \sigma_{12}\ \ \sigma_{21}\ \ \sigma_{13}\ \ \sigma_{31}\ \ \sigma_{23}\ \ \sigma_{32}\}^T \\ \{\delta\} &= \{1\ \ 1\ \ 1\ \ 0\ \ 0\ \ 0\ \ 0\ \ 0\ \ 0\}^T\end{aligned} \tag{1}$$

The applied stress vector is proportioned to each plane by multiplying related transitive matrix $[T_i]$ that are derived from the unit vectors. The following stress components are defined on each plane:

$$\begin{Bmatrix}\tau_1 \\ \tau_2 \\ \sigma_n\end{Bmatrix}_i = [T_i]\cdot\{\sigma\},\quad \tau = \sqrt{\tau_1^2+\tau_2^2} \tag{2}$$

where $[T_i]$ is defined as:

$$[T_i] = \begin{bmatrix} L_{x'_ix} & L_{x'_iy} & L_{x'_iz} \\ L_{y'_ix} & L_{y'_iy} & L_{y'_iz} \\ L_{z'_ix} & L_{z'_iy} & L_{z'_iz}\end{bmatrix}\cdot\begin{bmatrix} l_i & 0 & 0 & m_i & 0 & n_i & 0 & 0 & 0 \\ 0 & m_i & 0 & 0 & l_i & 0 & 0 & n_i & 0 \\ 0 & 0 & n_i & 0 & 0 & 0 & l_i & 0 & m_i\end{bmatrix} \tag{3}$$

The stress ratio of each plane is defined as follows:

$$\zeta = \frac{\tau}{\sigma_n} \tag{4}$$

3 PLASTICITY OF NEW MULTILAMINATE BOUNDING SURFACE CONSTITUTIVE MODEL

The plasticity of the new model is generally similar to the original model as proposed by Crouch et al. (1994) and follows the classic plasticity:

$$\{\dot{\varepsilon}\} = \{\dot{\varepsilon}^e\} + \{\dot{\varepsilon}^p\} \tag{5}$$

which states separate components of elastic $\{\varepsilon^e\}$ and plastic $\{\varepsilon^p\}$ strain vectors:

$$\begin{aligned}\{\dot{\varepsilon}\} &= [C^e]_T\cdot\{\dot{\sigma}\} + [C^p]_T\cdot\{\dot{\sigma}\} \\ [C^{ep}]_T &= [C^e]_T + [C^p]_T\end{aligned} \tag{6}$$

where $[C^e]$ and $[C^p]$ are defined for each plane as:

$$\begin{aligned}[C^e]_i &= \frac{1}{2G_i}[I] + \left(\frac{1}{9K_i} - \frac{1}{6G_i}\right)\cdot\{\delta\}\cdot\{\delta\}^T \\ [C^p]_i &= \frac{1}{H_i}\{Q\}_i\cdot\{P\}_i^T\end{aligned} \tag{7}$$

where, K_i and G_i are bulk and shear moduli at plane i. $\{Q\}$ and $\{P\}$ are defined as the unit normal to the loading surface and the unit direction of the plastic strain rate, respectively.

Table 1. Plane's unit vector components and weight coefficients for numerical integration.

Plane		1	2	3	4	5	6	7	8	9	10	11	12	13
Normal Axis	l_i	$\frac{\sqrt{3}}{3}$	$\frac{\sqrt{3}}{3}$	$-\frac{\sqrt{3}}{3}$	$-\frac{\sqrt{3}}{3}$	$\frac{\sqrt{2}}{2}$	$-\frac{\sqrt{2}}{2}$	$\frac{\sqrt{2}}{2}$	$-\frac{\sqrt{2}}{2}$	0	0	1	0	0
	m_i	$\frac{\sqrt{3}}{3}$	$-\frac{\sqrt{3}}{3}$	$\frac{\sqrt{3}}{3}$	$-\frac{\sqrt{3}}{3}$	$\frac{\sqrt{2}}{2}$	$\frac{\sqrt{2}}{2}$	0	0	$-\frac{\sqrt{2}}{2}$	$\frac{\sqrt{2}}{2}$	0	1	0
	n_i	$\frac{\sqrt{3}}{3}$	$\frac{\sqrt{3}}{3}$	$\frac{\sqrt{3}}{3}$	$\frac{\sqrt{3}}{3}$	0	0	$\frac{\sqrt{2}}{2}$	$\frac{\sqrt{2}}{2}$	$\frac{\sqrt{2}}{2}$	$\frac{\sqrt{2}}{2}$	0	0	1
w_i		$\frac{27}{840}$	$\frac{27}{840}$	$\frac{27}{840}$	$\frac{27}{840}$	$\frac{32}{840}$	$\frac{32}{840}$	$\frac{32}{840}$	$\frac{32}{840}$	$\frac{32}{840}$	$\frac{32}{840}$	$\frac{40}{840}$	$\frac{40}{840}$	$\frac{40}{840}$

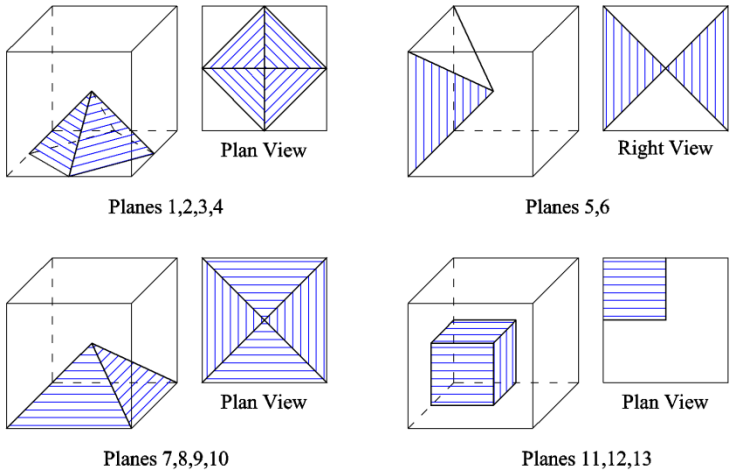

Figure 1. Planes used in the presented multilaminate constitutive model.

$[C^e]_T$ and $[C^p]_T$ are calculated based on numerical integration as follows:

$$[C^p]_T = 8\pi \cdot \sum_{i=1}^{13} w_i \cdot [C^e]_i$$
$$[C^e]_T = 8\pi \cdot \sum_{i=1}^{13} w_i \cdot [C^e]_i \quad (8)$$

The following 4 surfaces are defined in this constitutive model:

- Failure surface describing the critical state;
- Bounding surface recording the previous loading dominion and defining the plastic loading surface;
- Loading surface defining the direction of plastic loading; and,
- Plastic dilatancy surface, which is determined using the ratio of volumetric to deviatoric plastic strain.

3.1 Failure Surface

For simplicity, in the multilaminate model failure surface is assumed as Mohr-Coulomb form instead of the original elliptic form. This surface is specified by critical effective stress ratio, ζ_{cr}. The critical state line is shown in Figure 2.

3.2 Bounding Surface

The boundary surface includes three sectors: (1) a compressive ellipse, (2) a hyperbola and (3) a tensile ellipse as shown in Figure 2. The compressive elliptic part lies in $\sigma_{n_1} \le \sigma_n \le \sigma_{n_0}$ region where $\sigma_{n_1} = \sigma_{n_0}/R$. R is a material constant ($1 \le R < \infty$). σ_{n_0} varies as a function of the volumetric plastic strain and defines the size of bounding surface. The compressive ellipse meets the normal stress axis perpendicularly. The equation of the compressive ellipse is given as:

$$F = \bar{\tau} - \frac{N \cdot \sigma_{n_0}}{R}\sqrt{\left(1 - \left(\frac{\left(R\bar{\sigma}_n/\sigma_{n_0}\right) - 1}{R-1}\right)^2\right)} = 0 \quad (9)$$

N is the slope of a line passing from stress origin to the common tangent point of ellipse and hyperbola sectors. The hyperbola is located in $0 < \sigma_n < \sigma_{n_1}$ region and defined as:

$$F = \bar{\tau} - \frac{N \cdot \sigma_{n_0}}{R}\left(1 + \frac{AR}{N} - \sqrt{\left(1 - \frac{R\bar{\sigma}_n}{\sigma_{n_0}}\right)^2 + \left(\frac{AR}{N}\right)^2}\right) = 0 \quad (10)$$

The gap between N-line and the asymptote to the hyperbolic sector is controlled by $A \cdot \sigma_{n_0}$. The last sector is a tensile ellipse situated in $\sigma_{n_3} \le \sigma_n \le 0$ region and is defined as:

$$F = \bar{\tau} - \tau_r \sqrt{\left(1 - \left(1 - \frac{\bar{\sigma}_n - T\sigma_{n_0}}{\sigma_{n_r}}\right)^2\right)} = 0 \qquad (11)$$

$$\sigma_{n_r} = \frac{\sigma_{n_0} \cdot T^2 \cdot (\Psi / \tau_2)}{1 + 2\sigma_{n_0} \cdot T \cdot (\Psi / \tau_2)} \qquad (12)$$

$$\tau_r = \tau_2 \Big/ \sqrt{\left(1 - \left(1 + \left(T\sigma_{n_0} / \sigma_{n_r}\right)\right)^2\right)} \qquad (13)$$

$$\Psi = \frac{N}{\sqrt{\left(1 + (\mathrm{AR}/N)^2\right)}} \qquad (14)$$

$$\mathrm{J}_2 = \frac{N \cdot \sigma_{n_0}}{R}\left(1 + \frac{AR}{N} - \sqrt{\left(1 + (\mathrm{AR}/N)^2\right)}\right) \qquad (15)$$

3.3 Critical State Line, Normal Consolidation Line and Rebound Lines

In this model, the critical state, normal consolidation, and rebound lines are defined similar to what Crouch et al. (1994) defined by the exception that here the space is $e - Ln\sigma_n$ instead of $e - Ln\, I/3$.

3.4 Hardening/Softening Equation

The most crucial hardening/softening parameter is $\dot{\kappa}_{n_0}$ which defines the size of bounding surface (the intersection of compressive ellipse with normal stress axis). Variation in the amount of this parameter is a function of volumetric plastic strain as follows:

$$\dot{\kappa} = \dot{\kappa}_{n_0} = \frac{\left\langle \sigma_{n_0} - \sigma_l \right\rangle + \sigma_l}{\lambda + \kappa}(1 + e_{in}) \cdot \dot{\varepsilon}_v^p \qquad (16)$$

Moreover, elastic behavior of the model is not linear, and is a function of confining pressure. The elastic behavior is not transferred to the planes. The Bulk modulus follows the following hyper elastic formulation:

$$K = \frac{(1 + e_{in}) \cdot (\langle P - \sigma_l \rangle + \sigma_l)}{\kappa} \qquad (17)$$

P and σ_l are the average amount of principal stresses at the point, and model constant, respectively. σ_l represents a lower bound below which P does not have any effect on bulk and shear modules. By assuming a constant Poisson's ratio υ, tangent shear modulus can be defined as:

$$G = \frac{1.5K(1 - 2\nu)}{1 + \nu} \qquad (18)$$

3.5 Loading Surface

The stress point is always located on the loading surface that is defined based on the bounding surface using radial scaling method in the compressive elliptic sector ($\sigma_n > \sigma_{n_o} / R$) and deviatoric scaling method elsewhere ($\sigma_n \le \sigma_{n_o} / R$).

β is defined as the scaling coefficient and defined as:

$$\beta = \frac{\bar{\tau}}{\tau} \qquad (19)$$

However, in the case of isotropic loading (stress point on the σ_n axis) the it can be calculated as:

$$\beta = \left(\sigma_{n_0} \cdot (1/R - 1)\right) \Big/ \left(\sigma_{n_0} / R - \sigma_n\right) \qquad (20)$$

The loading surface equation in the radial scaling region is defined by substituting $(\sigma_{n_0} / R) + \beta(\sigma_n - (\sigma_{n_0} / R))$ for $\bar{\sigma}_n$ and $\beta\tau$ for $\bar{\tau}$ in the compressive sector of the bounding surface (Equation 9):

$$f = \beta\tau - \frac{N \cdot \sigma_{n_0}}{R}\sqrt{\left(1 - \left(\frac{\beta(R\sigma_n / \sigma_{n_0} - 1)}{R - 1}\right)^2\right)} = 0 \qquad (21)$$

The other two sectors of the loading surface are defined by replacing $\bar{\sigma}_n$ by σ_n for and $\bar{\tau}$ by $\beta\tau$ in Equations 10 and 11:

$$f = \beta\tau - \frac{N \cdot \sigma_{n_0}}{R}\left(1 + \frac{AR}{N} - \sqrt{\left(\left(1 - \frac{R\sigma_n}{\sigma_{n_0}}\right)^2 + \left(\frac{AR}{N}\right)^2\right)}\right) = 0 \qquad (22)$$

$$f = \beta\tau - \tau_r \sqrt{\left(1 - \left(1 - \frac{\sigma_n - T\sigma_{n_0}}{\sigma_{n_r}}\right)^2\right)} = 0 \qquad (23)$$

The direction of plastic loading vector could be obtained from the following equation:

$$\{Q\} = \frac{1}{\left|\{f_{,\sigma}\}\right|} \cdot \left(\underbrace{f_{,\sigma_n}\{\sigma_{ij}\}}_{\text{hydrostatic}} + \underbrace{f_{,\tau_{ij}}\{\tau_{ij}\}}_{\text{deviatoric}} \right) \qquad (24)$$

3.6 Plastic Dilatancy Surface and Plastic Strain Direction

Similar to the loading surface, plastic dilatancy surface is also passing through the stress point and geometrically similar to bounding surface; however, a different scaling method is used to define the plastic dilatancy surface from the bounding surface. In addition, there is dissimilarity in comparison to bounding surface regarding the compressive ellipse sector. The power of two in Equation

(9) is changed to n_g; thus, for $2 < n_g < \infty$ we have super-ellipse and for $1 < n_g < 2$ there is a sub-ellipse:

$$g = \tau - \frac{N_g \cdot \sigma_{n_0 g}}{R_g} \cdot \left(1 - \left(\frac{(R_g \sigma_n / \sigma_{n_{0g}} - 1)}{R_g - 1} \right)^{n_g} \right)^{\frac{1}{n_g}} = 0 \quad (25)$$

Despite of the fact that the bounding and plastic dilatancy surfaces are geometrically identical, the non-associated flow rule exists as the direction of loading increment vector differs from the direction of the plastic strain increment vector. The direction of plastic strain vector can be evaluated as:

$$\{P\} = \frac{1}{\left| \{g_{,\sigma}\} \right|} \cdot \left(g_{,\sigma_n} \cdot \{\sigma_{n,\sigma}\} + f_{,\tau} \cdot \{\tau_{,\sigma}\} \right) \quad (26)$$

The surfaces described above are schematically shown in Figure 2.

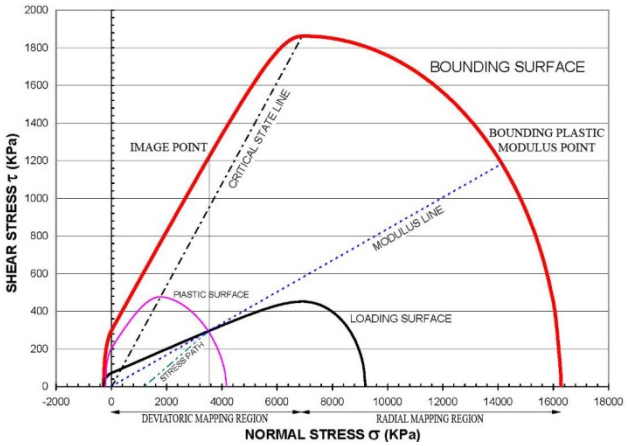

Figure 2. Schematic presentation of the different surfaces in bounding surface model.

4 SENSITIVITY OF MATERIAL PARAMETERS

The original constitutive model presented by Crouch et al. (1994) is defined by 32 parameters. Crouch et al. (1994) stated that in majority of practical cases only 8 parameters are to be defined and default values may be considered for the remaining 24 material parameters. Basically, although the values of some of the material parameters are different when the constitutive model is described in the multilaminate framework, the role of the material parameters on prediction of stress-strain behavior of soils are the same.

In this article, a sensitivity analysis has been performed to describe the effects of the most important material parameters in the multilaminate model and initial stress condition on prediction of stress-strain behavior of granular soils in drained and undrained conditions and to highlight the capabilities and flexibility of the proposed model. Table 2 presents the definition of these material parameters.

Table 2. Material parameters used in sensitivity analysis.

Material Parameter Definition	symbol
Critical state line slope in e-Lnσ_n space	λ
Slope of unloading line in e-Lnσ_n space	κ
Critical state void ratio	e_{crk}
Critical state line slope in σ_n - τ space	ζ_{crc}
Parameter for size of boundary surface	A_c
Initial void ratio	e_{in}
Initial mean stress (initial stress state)	σ_{no}

Figures 3 to 9 present the effect of variation of the parameters stated in Table 2 on drained and undrained behavior of a sand.

5 SUMMARY

A new constitutive model in multilaminate framework is presented for granular materials. This paper discussed the constitutive equations of the model based on a non-linear elastic behavior and plastic behavior at the predefined planes from multilaminate framework.

Further, a sensitivity analysis was carried out to show the flexibility of this model in prediction of stress-strain behavior of granular materials in drained and undrained conditions.

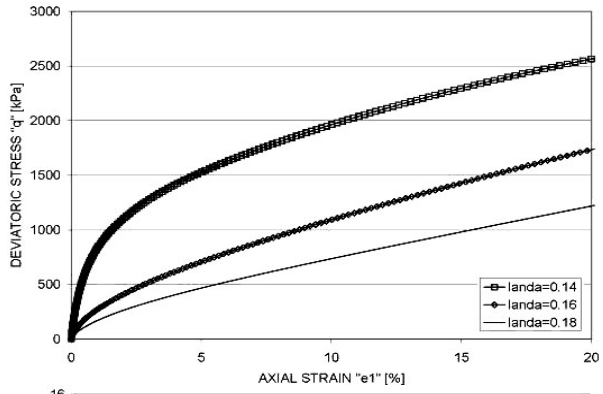

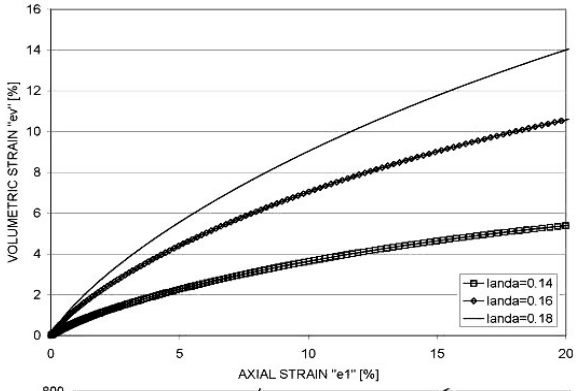

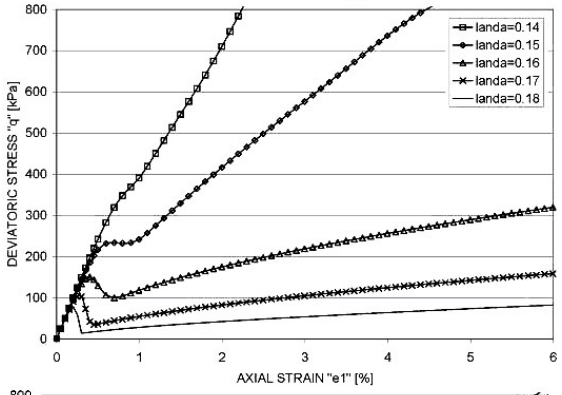

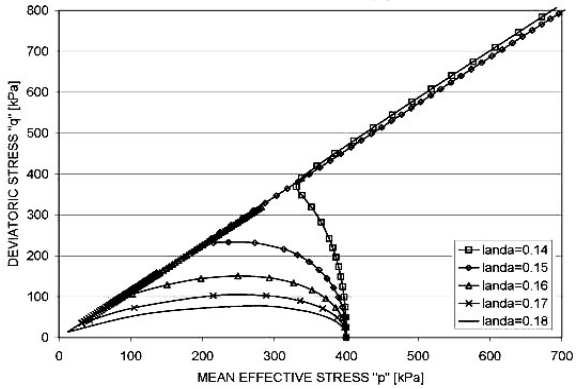

Figure 3. Effects of parameter λ on a) drained stress-strain behavior, b) drained volumetric behavior, c) undrained stress-strain behavior, d) mean effective stress versus deviator stress.

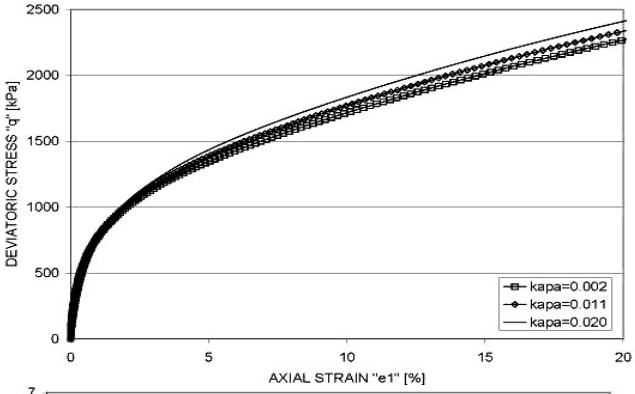

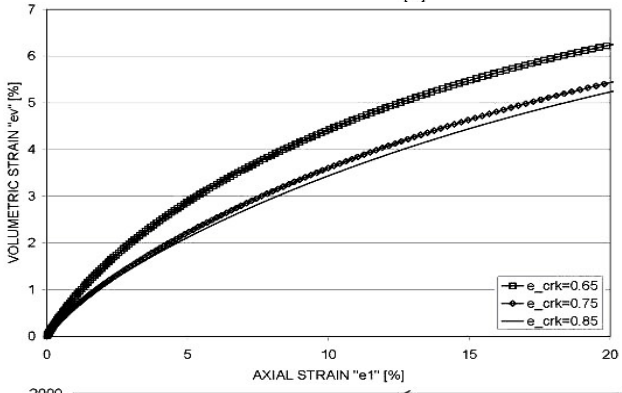

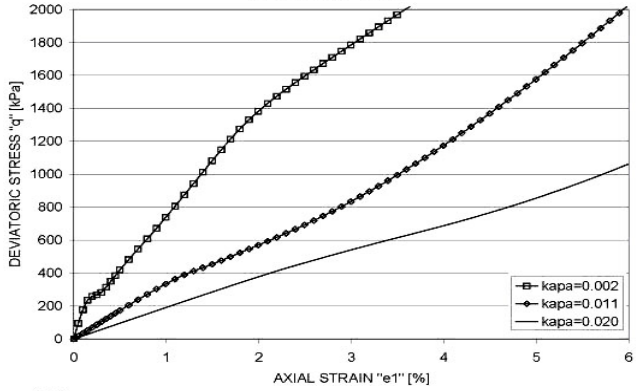

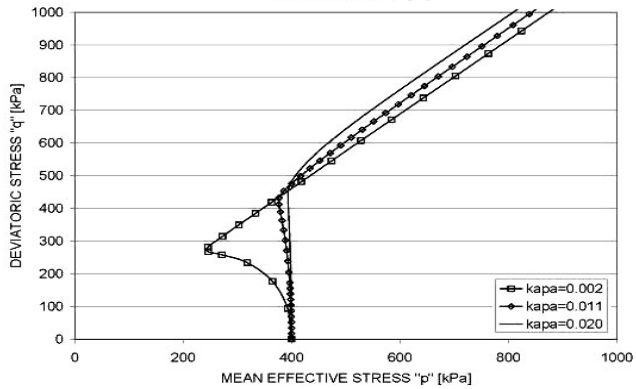

Figure 4. Effects of parameter κ on a) drained stress-strain behavior, b) drained volumetric behavior, c) undrained stress-strain behavior, d) mean effective stress versus deviator stress.

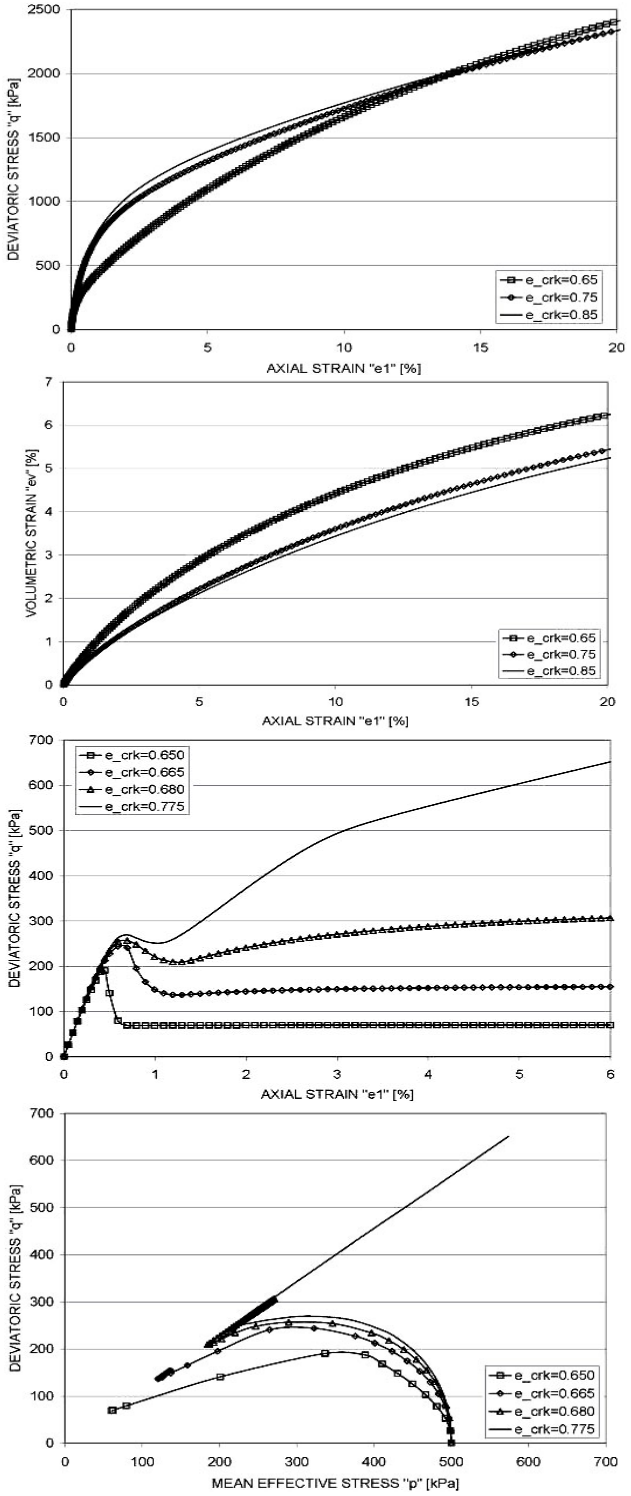

Figure 5. Effects of parameter e_{crk} on a) drained stress-strain behavior, b) drained volumetric behavior, c) undrained stress-strain behavior, d) mean effective stress versus deviator stress.

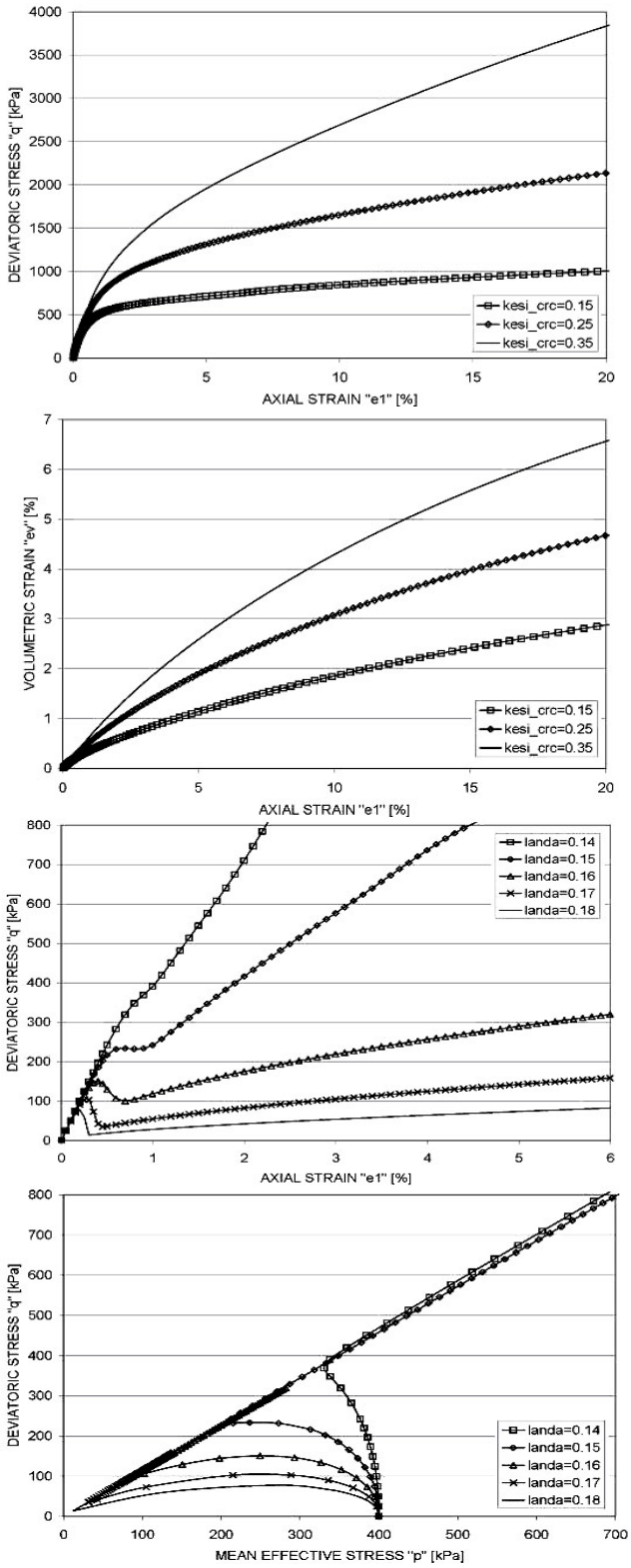

Figure 6. Effects of parameter ζ_{crc} on a) drained stress-strain behavior, b) drained volumetric behavior, c) undrained stress-strain behavior, d) mean effective stress versus deviator stress.

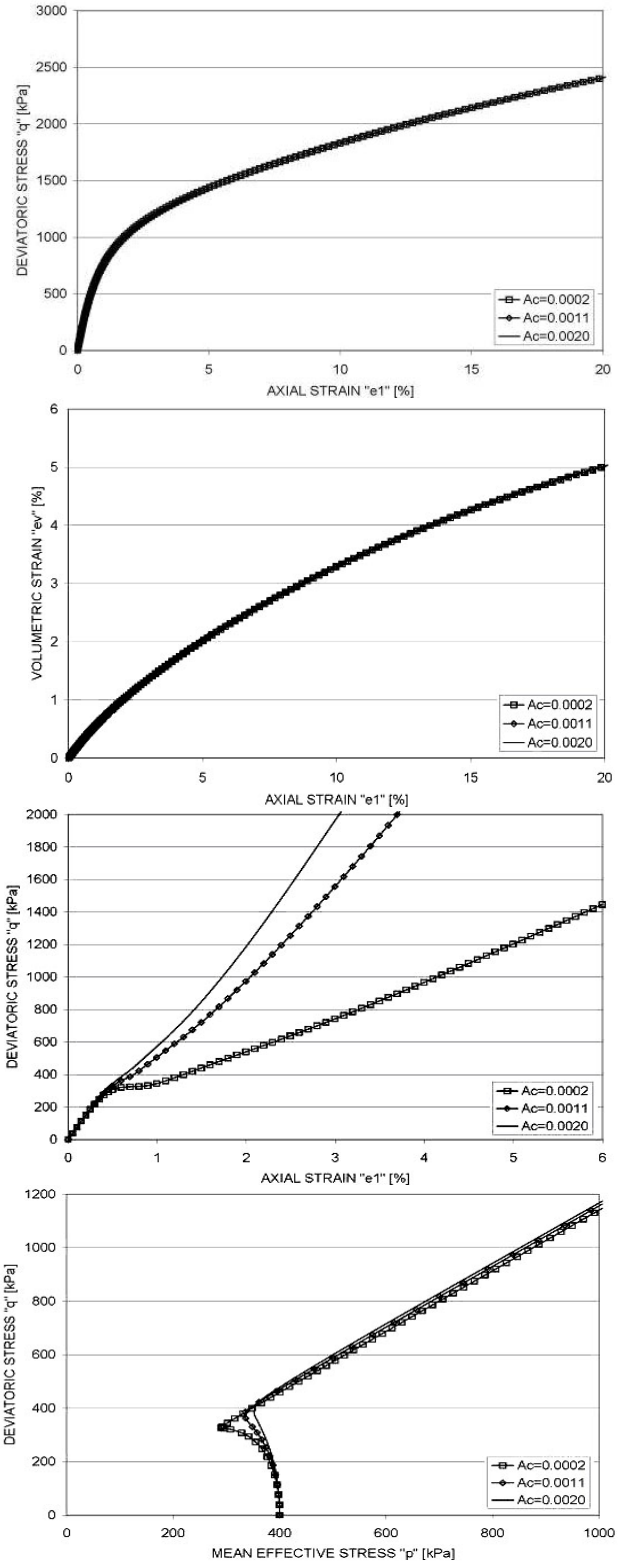

Figure 7. Effects of parameter A_c on a) drained stress-strain behavior, b) drained volumetric behavior, c) undrained stress-strain behavior, d) mean effective stress versus deviator stress.

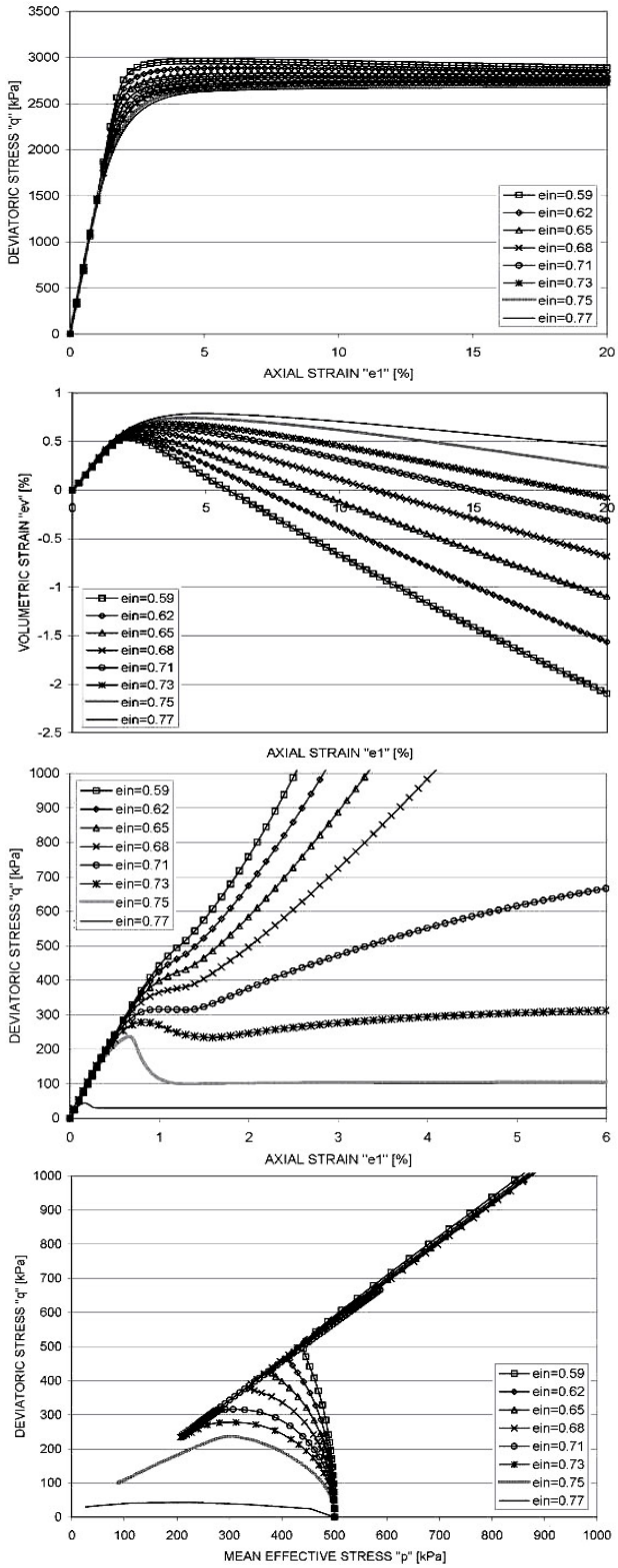

Figure 8. Effects of parameter e_{in} on a) drained stress-strain behavior, b) drained volumetric behavior, c) undrained stress-strain behavior, d) mean effective stress versus deviator stress.

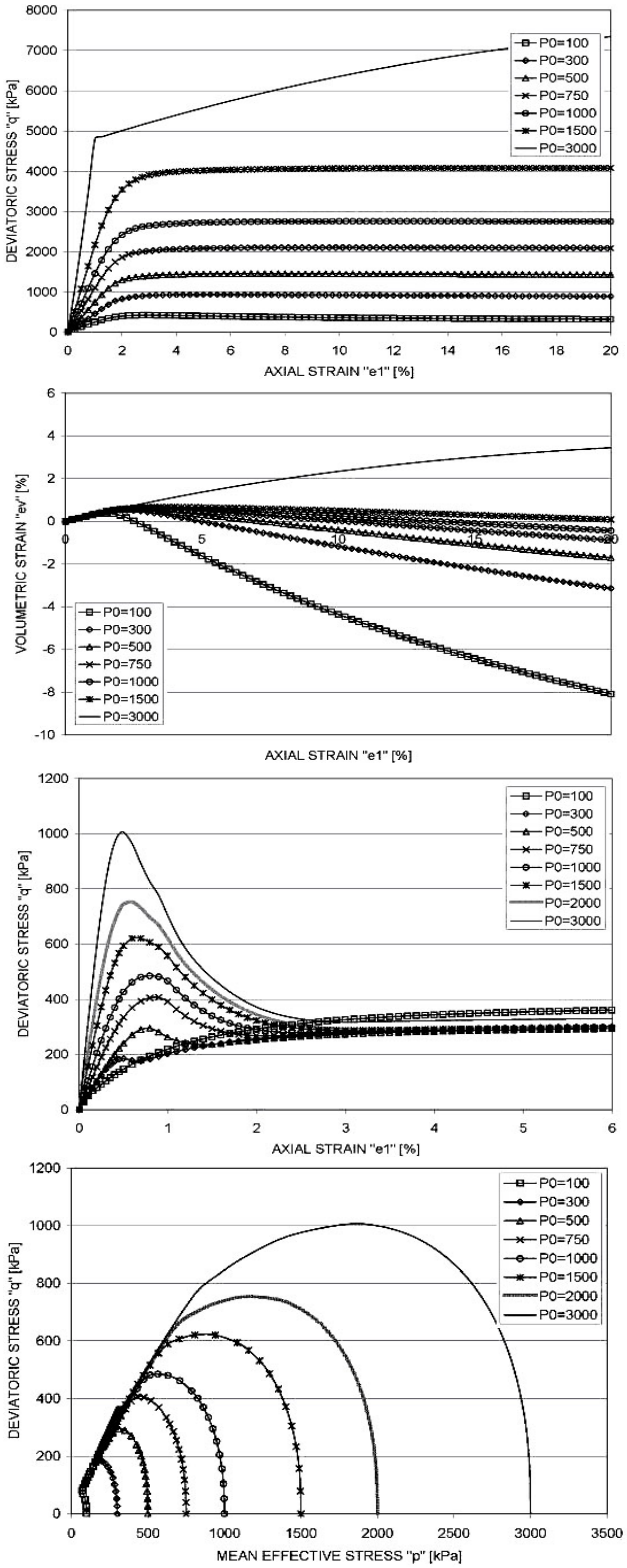

Figure 9. Effects of parameter σ_{no} on a) drained stress-strain behavior, b) drained volumetric behavior, c) undrained stress-strain behavior, d) mean effective stress versus deviator stress.

6 REFERENCES

Drucker, D.C., Gibson, R.E., and Henkel, D.I. 1957. Soil mechanics and work-hardening theories of plasticity. Trans., ASCE, 122, 338-346.

Roscoe, K.H., and Burland, J.B. 1968. On the generalized stress-strain behaviour of 'wet' clay. Engineering Plasticity. J. Heymann and F. A. Leckie, eds., Cambridge University Press, Cambridge, England, 535-609.

DiMaggio, F.L. and Sandler, I.S. 1971. Material model for granular soils. Journal of Engineering Mechanics Div., ASCE, 97 (3), 935-950.

Lade, P.V. 1977. Elasto-plastic stress-strain theory for cohesionless soil with curved yield surfaces. International Journal of Solids Structure, 13, 1019-1035.

Prevost, J-U. 1978. Plasticity theory for soil stress-strain behavior. Journal of Engineering Mechanics Div., ASCE, 104 (5), 1177-1194.

Mroz, Z., Norris, V.A., and Zienkiewicz, O.C. 1981. An anisotropic, critical state model for soils subjects to cyclic loading. Geotechnique, London, England, 31 (4), 451-469.

Ghaboussi, J. and Momen, H., 1982. Modeling and analysis of cyclic behavior of sands, G. N. Pande and O. C. Zienkiewicz (eds), Soil Mechanics-Transient and Cyclic Loads, Wiley, New York, 313-342.

Desai, C.S., and Faruque, M.O. 1984. Constitutive model for (geological) materials.' Journal of Engineering Mechanics, ASCE, 110 (9), 1391-1408.

Poorooshasb, H.B. and Pietruszczak, S. 1985. On yielding and flow of sand; a generalized two-surface model, Computers and Geomechanics, 1, 33-58.

Dafalias, Y.F. and Herrmann, L.R. 1986. Bounding surface plasticity. II: Application to isotropic cohesive soils, Journal of Engineering Mechanics, 112 (12), 1263-1291.

Frantziskonis, G., Desai, C.S., and Somasundaram, S. 1986. Constitutive model for non-associative behavior. Journal of Engineering Mechanics, ASCE, 112 (9), 932-946.

Crouch, R.S. and Wolf, J.P. 1994. Unified 3D Critical State Bounding Surface Plasticity Model for Soils Incorporating Continuous Plastic Loading under Cyclic Paths. Part I: Constitutive relations, International Journal of Numerical and Analytical Methods in Geomechanics, 18, 735-758.

Taylor G.I. 1938. Plastic strain in metals. Journal of Industrial Metals, 62, 307-324.

Batdorf S.B. and Budiansky B. 1949. A mathematical theory of plasticity based on the concept of slip. National advisory committee for Aeronautics, T1871.

Zienkiewicz, O.C., Pande G.N. 1977. Time-dependent Multilaminate model of rocks - a numerical study of deformation and failure of rock masses, International Journal of Numerical and Analytical Methods in Geomechanics, 1 (3), 219-247.

Pande G.N. and Piretruszczak S. 1982. Reflecting surface model for soils, proceeding International Symposium Numerical Methods in Geomechanics, Zurich, A.A. Balkema, Rotterdam, 50-64.

Pande G.N. and Sharma K.G. 1983. Multilaminate model of clays, International Journal of Numerical and Analytical Methods in Geomechanics, 7 (4), 397-418.

Bazant Z.P. and Oh B.H. 1983. Micro plane model for fracture analysis of concrete structures, Proceeding Symposium on the interaction of Non-nuclear munitions with structures, published by McGregor & Werner, Washington.

Pietruszczak S. and Pande G.N. 2001. Description of soil anisotropy based on multi-laminate framework. Int. journal for numerical and analytical methods in geomechanics. Vol. 25, pp 197-206

Sadrnejad S.A., Karimpour H. 2010. A Bounding Surface Model for Sand Behaviour under Drained and Undrained Conditions, International Journal of Civil Engineering 9 (2), 96-110.

Schweiger, H.F., Wiltafsky, C., Scharinger, F. and Galavi, V. 2009. A multilaminate framework for modelling induced and inherent anisotropy of soils. Geotechnique 59 (2), 87-101.